Red Fluorescent Protein from *Discosoma* as a Fusion Tag and a Partner for Fluorescence Resonance Energy Transfer†

Hideaki Mizuno,‡ Asako Sawano,‡,§ Pharhad Eli,‡ Hiroshi Hama,‡ and Atsushi Miyawaki*,‡

Laboratory for Cell Function and Dynamics, Advanced Technology Development Center, Brain Science Institute, The Institute of Physical and Chemical Science (RIKEN), 2-1 Hirosawa, Wako-city, Saitama, 351-0198, Japan, and Brain Science Research Division, Brain Science and Life Technology Research Foundation, 1-28-12 Narimasu, Itabashi, Tokyo, 175-0094, Japan

Received September 26, 2000; Revised Manuscript Received November 28, 2000

ABSTRACT: The biochemical and biophysical properties of a red fluorescent protein from a *Discosoma* species (DsRed) were investigated. The recombinant DsRed expressed in *E. coli* showed a complex absorption spectrum that peaked at 277, 335, 487, 530, and 558 nm. Excitation at each of the absorption peaks produced a main emission peak at 583 nm, whereas a subsidiary emission peak at 500 nm appeared with excitation only at 277 or 487 nm. Incubation of *E. coli* or the protein at 37 °C facilitated the maturation of DsRed, resulting in the loss of the 500-nm peak and the enhancement of the 583-nm peak. In contrast, the 500-nm peak predominated in a mutant DsRed containing two amino acid substitutions (Y120H/K168R). Light-scattering analysis revealed that DsRed proteins expressed in *E. coli* and HeLa cells form a stable tetramer complex. DsRed in HeLa cells grown at 37 °C emitted predominantly at 583 nm. The red fluorescence was imaged using a two-photon laser (Nd:YLF, 1047 nm) as well as a one-photon laser (He:Ne, 543.5 nm). When fused to calmodulin, the red fluorescence produced an aggregation pattern only in the cytosol, which does not reflect the distribution of calmodulin. Despite the above spectral and structural complexity, fluorescence resonance energy transfer (FRET) between *Aequorea* green fluorescent protein (GFP) variants and DsRed was achieved. Dynamic changes in cytosolic free Ca^{2+} concentrations were observed with red cameleons containing yellow fluorescent protein (YFP), cyan fluorescent protein (CFP), or Sapphire as the donor and RFP as the acceptor, using conventional microscopy and one- or two-photon excitation laser scanning microscopy. Particularly, the use of the Sapphire−DsRed pair rendered the red cameleon tolerant of acidosis occurring in hippocampal neurons, because both Sapphire and DsRed are extremely pH-resistant.

Green fluorescent proteins (GFPs)[1] are found in a large number of bioluminescent coelenterates (*1*). GFPs were thought to be an accessory emitter protein of the cnidarian luminescent system, deriving their excitation by nonradiative energy transfer in association with the luciferase reaction. The GFP from *Aequores victoria* (*Aequorea* GFP) is now widely used in molecular and cellular biology studies (*2*). However, several GFP-like fluorescent proteins have been isolated from fluorescent but nonbioluminescent Anthozoa species (*3*). Among them is a red-emitter peaking at 583 nm, called DsRed or drFP583. Although the GFP-like fluorescent proteins have only 26−30% sequence identity with *Aequorea* GFP, several features of GFP structure are probably conserved, including the "β-can" fold.

Since DsRed has longer wavelengths of excitation and emission than are currently available from *Aequorea* GFP, it would be useful for multi labels and reporters and could serve as a resonance energy transfer acceptor. However, complicated features in its spectra and structure have been pointed out, which limit the usefulness of DsRed as a tool. First, the absorption spectrum of DsRed is broad with several shoulders and peaks other than the main peak at 558 nm. Also, a small peak at 500 nm in the emission spectrum is mentioned in the manufacturer's brochure (Clontech). Second, a spotty pattern of red fluorescence has often been observed when DsRed was fused to a certain protein and expressed in eukaryotic cells, suggesting aggregation of the chimera protein.

Spectral and structural features of fluorescent proteins are generally dependent on each other. With the exception of *Aequorea* GFP, all GFP molecules so far studied have been

† This work was partly supported by grants from CREST of JST (Japan Science and Technology) and the Japanese Ministry of Education, Science and Culture.

* To whom correspondence should be addressed at the Laboratory for Cell Function and Dynamics, Advanced Technology Development Center, Brain Science Institute, The Institute of Physical and Chemical Science (RIKEN); 2-1 Hirosawa, Wako-city, Saitama, 351-0198, Japan. Tel +81-48-467-5917; Fax +81-48-467-5924; E-mail matsushi@brain.riken.go.jp.

‡ The Institute of Physical and Chemical Science (RIKEN).

§ Brain Science and Life Technology Research Foundation.

[1] Abbreviations: $[Ca^{2+}]_c$, calcium concentration in the cytosol; CaM, calmodulin; CBB, Coomassie brilliant blue R250; CFP, cyan fluorescent protein; CRC2, cyan red cameleon-2; DsRed, red fluorescent protein cloned from *Discosoma* coral; DTT, dithiothreitol; ECFP, enhanced cyan fluorescent protein; EYFP-V68L/Q69K, enhanced yellow fluorescent protein that is less pH-sensitive; FRET, fluorescence resonance energy transfer; GFP, green fluorescent protein; IPTG, isopropyl-β-D-thiogalactopyranoside; MALS, multi-angle light scattering; RT, room temperature; Sapphire, ≡H9-40 which has mutations S72A/Y145F/T203I; SapRC2, Sapphire red cameleon-2; SDS−PAGE, sodium dodecyl sulfate−polyacrylamide gel electrophoresis; TTX, tetrodotoxin; YFP, yellow fluorescent protein; YRC2, yellow red cameleon-2.

10.1021/bi002263b CCC: $20.00
Published on Web 02/01/2001

stable nondissociable dimers in diluted aqueous solution (*4*). In contrast, *Aequorea* GFP forms a dimeric complex but only at a high protein concentration. It is of interest that wild-type *Aequorea* GFP undergoes large changes in its absorption spectrum upon dimerization (*5*). In the present study, we investigated the inter-relationships between the structure and spectra of DsRed in hopes of achieving better use of the fluorescent protein as a fusion tag and a partner for fluorescence resonance energy transfer (FRET).

Cameleons are chimeric proteins consisting of a blue or cyan mutant of GFP, calmodulin (CaM), a glycylglycine linker, the CaM binding peptide of myosin light chain kinase (M13), and a green or yellow version of GFP (*6*). Ca^{2+} binding to the CaM causes intramolecular CaM binding to M13. The resulting change from an extended to a more compact conformation increases the efficiency of FRET between the shorter to the longer wavelength mutant GFP. To obtain adequate expression and brightness of the mutant GFPs in mammalian cells, enhanced genes with mammalian codon usage and mutations for improved folding at 37 °C were developed. Also the blue mutant (BFP) proved to be the dimmest and most bleachable of the GFPs. It also required ultraviolet excitation, which is potentially injurious, excites the most cellular autofluorescence, and could interfere with the use of caged compounds. Therefore, enhanced cyan and yellow mutants, ECFP and EYFP, have been substituted for the original blue and green mutants, respectively, to make "yellow cameleons". Despite the considerable promise of yellow cameleons, they still have problems that need amelioration. One of the problems is that EYFP is quenched by acidification. This problem perturbed the signals of yellow cameleons, mimicking a decrease in $[Ca^{2+}]$ when the cellular environment acidified. The pH-sensitivity of yellow cameleons has been greatly reduced by introducing mutations V68L and Q69K into EYFP (EYFP-V68L/Q69K) (*7*). The improved yellow cameleons, including yellow cameleon-2.1, permit Ca^{2+} measurements without perturbation by pH changes from 6.5 to 8.0. Mutations have been also introduced into the Ca^{2+} binding loops of CaM to tune the affinity of yellow cameleons for Ca^{2+}. Herein, we experimented with three pairs: YFP−DsRed, CFP−DsRed, and Sapphire−DsRed for cameleons [Sapphire is a GFP variant (≡H9-40) containing a mutation of Thr203 to Ile, which results in a stabilization of the neutral form of the chromophore (*8*)]. Features of the resulting "yellow-red cameleons", "cyan-red cameleons", and "Sapphire-red cameleons" will be discussed.

EXPERIMENTAL PROCEDURES

Recombinant DsRed Expressed in E. coli. The gene for DsRed was amplified by polymerase chain reaction (PCR) using pDsRed1-1 (Clontech) as a template with a forward primer containing a *Bam*HI site and a reverse primer containing an *Eco*RI site. The restricted product was cloned in-frame into the *Bam*HI/*Eco*RI sites of $pRSET_B$ (Invitrogen). The resulting plasmid DNA, DsRed/$pREST_B$, encoded DsRed with an Xpress tag at the N-terminus. DsRed-mu43 was obtained by PCR-based random mutagenesis (*9*). Expression of the recombinant DsRed in *E. coli* and its purification were carried out as previously reported (*3*, *10*). The temperature and time of incubation after addition of isopropyl-β-D-thiogalactopyranoside (IPTG) were changed for optimization of the expression. Purity of the protein sample was checked by sodium dodecyl sulfate−polyacrylamide gel electrophoresis (SDS−PAGE) followed by Coomassie brilliant blue R250 (CBB) staining. Protein concentration was determined using a protein assay kit (Bio-Rad) using bovine serum albumin (BSA) as a standard. Absorption, emission, and excitation spectra were acquired in 50 mM HEPES, pH 8, using a U3310 spectrophotometer (Hitachi, Tokyo, Japan) and a F2500 fluorescence spectrophotometer (Hitachi). For size-exclusion chromatography, Superdex 200HR10/30 (Amersham Pharmacia) was installed on ÄKTA explorer 10S (Amersham Pharmacia), and fluorescence was monitored with an RF-10AXL fluorescence detector (Shimadzu, Kyoto, Japan). The Xpress tag was liberated from DsRed expressed in *E. coli* by incubation with recombinant enterokinase (2 units/100 μg of protein, Novagen), at 20 °C for 20 h. Multi-angle light scattering (MALS) was measured with a multi-angle light photometer (DAWN, Wyatt, Santa Barbara, CA) connected to a Shodex HPLC system (Showa Denko, Tokyo, Japan) on which size-exclusion columns (tandem connection of KW-804 and KW-803, Showa Denko) were installed (*11*).

Expression of DsRed in HeLa Cells. The DsRed gene was amplified by PCR with a sense primer containing a *Hin*dIII site and kozak consensus sequence (TCCACCATG), and a reverse primer containing an *Eco*RI site. The restricted fragment was inserted into the *Hin*dIII/*Eco*RI sites of pcDNA3 (Invitrogen) to construct DsRed/pcDNA3. HeLa cells were grown on a 10-cm tissue culture dish to 40% confluence in Dulbecco's modified Eagle's medium (Sigma) with 10% fetal bovine serum (Sigma), and transfected with 4 μg/dish of DsRed/pcDNA3 using lipofectin (GIBCO). One to three days after the transfection, the dish was placed on ice for 10 min, and then cells were washed twice in 10 mL of phosphate-buffered saline. Cell extract was prepared by incubating cells for 5 min on ice in 500 μL of lysis buffer (1% Triton X-100, 50 mM HEPES−NaOH, pH 8.0) supplemented with 50 μM phenylmethylsulfonyl fluoride, 10 μM leupeptin, 10 μM E-64, and 1 μM pepstatin A. The lysate was used for size-exclusion chromatography. Eluate was fractionated and subjected to SDS−PAGE followed by immunoblotting. DsRed on a membrane was detected using a living colors D.s. peptide antibody (Clontech) and an ECL detection system (Amersham Pharmacia).

Acquisition of Fluorescence Images of HeLa Cells Expressing ECFP and DsRed with Two-Photon Excitation Laser Scanning Microscopy. HeLa cells were grown on a 35-mm glass-bottom dish and cotransfected with 1 μg/dish of DsRed/pcDNA3 and ECFP/pcDNA3. ECFP−CaM/pcDNA3 was described previously (*6*). The gene for full-length DsRed was amplified by PCR, and was substituted for the ECFP gene to create DsRed−CaM/pcDNA3. Cells were observed with a two-photon laser scanning microscope based on a Fluoview FV500 scanning unit (Olympus, Tokyo, Japan) and two pulse lasers: a Ti:sapphire laser (Tsunami; Spectra Physics, Mountain View, CA) and an Nd:YLF laser (DPM-1000PC; Coherent Scotland, Glasgow, Scotland). The objective lens used was UPlanAPO 60xW/IR (Olympus). ECFP and DsRed were excited at 800 nm with the Ti:sapphire laser and at 1047 nm with the Nd:YLF laser, respectively. Excitation beams from the two lasers were alternately irradiated to the sample. Fluorescence was detected through band-pass filters BA465-495 (Olympus) and

Table 1: Filters and Dichroic Mirrors Used To Acquire Images of Neurons Expressing Red Cameleons with Conventional Fluorescence Microscopy[a]

	YRC2	CRC2	SapRC2
Ex. filter	480DF10	440DF20	400DF15
dichroic mirror	505DRLP	455DRLP	455DRLP
Em. filter, donor	535DF25	480DF30	510WB40
Em. filter, acceptor	565EFLP	565EFLP	565EFLP

[a] All filters and mirrors were purchased from Omega.

Table 2: Lasers, Filters, and Dichroic Mirrors Used To Acquire Images of HeLa Cells Expressing Red Cameleons with Laser Scanning Microscopy

	YRC2	CRC2	SapRC2
Ex. wavelength	488 nm[a]	800 nm[b]	770 nm[b]
dichroic mirror	DM351/488[c]	RDM650[c] & DM650[c]	RDM650[c] & DM650[c]
IR cut filter		BA650RIF[c]	BA650RIF[c]
beam splitter	SDM560[c]	DM505[c]	560DRLP
Em. filter, donor	BA515-550[c]	BA465-495[c]	510WB40
Em. filter, acceptor	BA560IF[c]	590DF35	580DF30

[a] Argon-ion laser (Omnichrome, Melles Griot). [b] Ti: sapphire laser (Tsunami, Spectra Physics). [c] Filters and mirrors obtained from Olympus. Others were from Omega.

590DF35 (Omega) for ECFP and DsRed, respectively. ECFP and DsRed fused to CaM were observed using the same instruments.

Dissociation Culture of Hippocampal Neurons. Primary neurons were prepared from Wistar rat embryos (E17-18) according to references (*12*, *13*). Calcium phosphate precipitation was used to transfect the neurons (*14*).

Calcium Imaging Using Red Cameleons. The cDNAs of all red cameleons were constructed from the cDNA of yellow cameleon-2.1, one of the improved yellow cameleons that have EYFP-V68L/Q69K. CRC2 (cyan red cameleon-2) was made by substituting DsRed for EYFP-V68L/Q69K. In addition to the substitution, replacement of ECFP with EYFP-V68L/Q69K and Sapphire produced YRC2 (yellow red cameleon-2) and SapRC2 (Sapphire red cameleon-2), respectively. HeLa cells and hippocampal neurons were transfected with mammalian expression vectors containing the genes for YRC2, CRC2, and SapRC2. They were imaged using the optical apparatus described in Table 1 (conventional microscopy) and Table 2 (one- or two-photon excitation laser scanning microscopy). The conventional microscopy system had a 75-W xenon lamp, an inverted microscope (IX 70, Olympus), a cooled CCD camera (MicroMax, Roper Scientific), and a filter changer (Lambda 10-2, Sutter Instruments) to alternate two emission filters for dual-emission ratio imaging. These instruments were controlled by MetaFluor 4.0 software (Universal Imaging).

RESULTS

Expression of DsRed in E. coli, and the Absorption and Emission Spectra. DsRed fused with Xpress tag (Invitrogen) at the N-terminus was expressed in *E. coli*. The tag contains six histidines followed by an enterokinase cleavage site; its molecular mass is 3.5 kDa. The temperature and time of *E. coli* incubation after addition of IPTG were optimized for efficient production of DsRed. Four different conditions [at room temperature (RT) or 37 °C, for 24 or 75 h] are listed in Table 3. DsRed was recovered from the medium as well as the cell lysate, since the fluorescence appeared also in the culture medium except at RT for 24 h, suggesting a warmer temperature to facilitate secretion of DsRed into the medium. DsRed with the tag was purified with a Ni−NTA column to a single band on SDS−PAGE (data not shown). We found that longer incubation at a warmer temperature yielded more red fluorescence in both bacteria and the medium. By contrast, *Aequorea* GFP is more abundantly expressed at lower temperatures and accumulates inside cells; incubation at RT for 24 h should usually yield sufficient production of *Aequorea* GFP.

Table 3: Expression of DsRed in *E. coli*

sample	condition after IPTG addition: temp	condition after IPTG addition: time (h)	prepared from	amount of DsRed (mg/100 mL of culture)	F_{500}/F_{580} (%)
$DsRed_{RT,24,p}$	RT	24	cells	9	61
$DsRed_{RT,75,p}$	RT	75	cells	4	13
$DsRed_{RT,75,s}$	RT	75	supernatant	15	9
$DsRed_{37,24,p}$	37 °C	24	cells	13	14
$DsRed_{37,24,s}$	37 °C	24	supernatant	6	12
$DsRed_{37,75,p}$	37 °C	75	cells	4	6
$DsRed_{37,75,s}$	37 °C	75	supernatant	24	5

Figure 1A shows absorption and emission spectra of $DsRed_{RT,24,p}$. The absorption spectrum was broad with five peaks at wavelengths of 277, 335, 487, 530, and 558 nm. It differed slightly from that reported by Matz et al. (*3*); the 277-nm and 487-nm peaks showed relatively higher amplitudes in the spectrum of $DsRed_{RT,24,p}$ than in the spectrum previously reported (*3*). Since the absorbance at 277 nm represents the quantity of the purified protein, it suggested that the chromophore was less formed in the $DsRed_{RT,24,p}$ sample. Next, the emission spectrum of $DsRed_{RT,24,p}$ was obtained by excitation at the wavelength of each of the absorption peaks. When excited at 558, 530, or 335 nm, a peak appeared at 583 nm on the emission spectrum. In contrast, excitation of the protein sample at 487 or 277 nm gave rise to a minor peak at 500 nm in addition to the 583-nm peak.

We noticed that a larger amount of red fluorescence was produced by incubated cells at a higher temperature and for a longer period. We suspected that better expression of DsRed resulted in a different spectral property. Therefore, we examined the spectra of $DsRed_{37,75,s}$ (Figure 1B). The absorption spectrum corresponded well with that reported by Matz et al. (*3*). The 277-nm and 487-nm peaks were less significant in $DsRed_{37,75,s}$ than in $DsRed_{RT,24,p}$. Again, the emission spectra of $DsRed_{37,75,s}$ were obtained by excitation at the absorption peaks. The minor peak at 500 nm was essentially missing, when $DsRed_{37,75,s}$ was excited at 277 and 487 nm. These results suggested the presence of a subcomponent of fluorescence, which was excited at 277 and 487 nm and emitted at 500 nm, and which resided transiently in DsRed during its maturation.

Figure 1D and 1E show the excitation spectra of $DsRed_{RT,24,p}$ and $DsRed_{37,75,s}$, respectively, with an emission wavelength of 583 nm. Also the excitation spectrum of $DsRed_{RT,24,p}$ with the emission at 500 nm is shown in Figure 1D; there were two excitation peaks around 280 and 460 nm. Excitation of $DsRed_{RT,24,p}$ at 460 nm gave both the major (583 nm) and the minor (500 nm) emission peaks. The ratio of peak

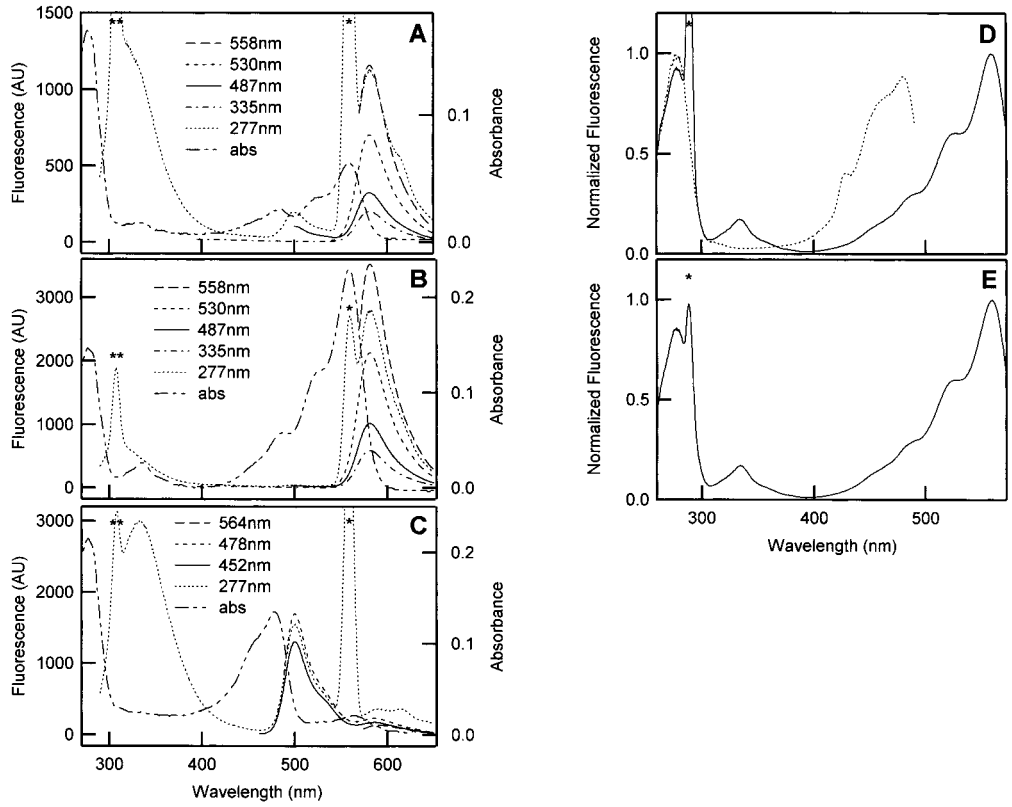

FIGURE 1: (A−C) Absorption and emission spectra of $DsRed_{RT,24,p}$ (A), $DsRed_{37,75,s}$ (B), and DsRed-mu43 (C). The emission spectra were obtained with excitation at the wavelengths denoted. (D and E) Excitation spectra of $DsRed_{RT,24,p}$ (D) and $DsRed_{37,75,s}$ (E) acquired with emission wavelengths of 583 nm (solid line) and 500 nm (D, dotted line). Excitation spectra were normalized with the highest value of the respective spectra. The Raman peaks from water are indicated by **, and the peaks due to scattering of the excitation light by *.

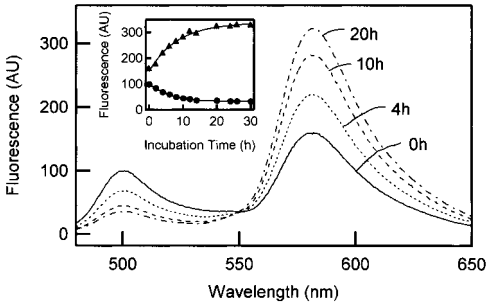

FIGURE 2: Time-dependent changes in emission spectra of $DsRed_{RT,24,p}$ by incubation at 37 °C. Emission spectra were obtained by excitation at 460 nm. Inset: Peak heights at 500 (circles) and 580 (triangles) nm on the spectra are plotted against incubation time. They were fitted with exponential curves, and τ values were estimated to be 6.3 and 8.4 h, respectively.

amplitudes at 500 to 583 nm ($R_{500/583}$) was low when DsRed was produced at 37 °C and for 75 h, and was prepared from the medium. Assuming that there is a transition from the subcomponent emitting at 500 nm to the main component at 583 nm during maturation of DsRed, we attempted to mature $DsRed_{RT,24,p}$. Incubation of $DsRed_{RT,24,p}$ at 37 °C resulted in a 68% reduction of the 500-nm peak with a 107% increase in the 583-nm peak, and thus $R_{500/583}$ decreased from 61% to 10% (Figure 2). The temporal profiles of the decrease and increase were fitted with exponential curves with similar τ values: 6.3 and 8.4 h, respectively (Figure 2, inset). In addition, all of the spectra passed through an isosbestic point (Figure 2). These results suggested a simple two-state mechanism for the transition.

The presence of the subcomponent was further verified by obtaining a mutant DsRed (DsRed-mu43) which emitted principally at 500 nm. DsRed-mu43 carried two amino acid substitutions (Y120H/K168R). DsRed-mu43 absorbed at 277, 452, 478, and 564 nm (Figure 1C), but not around 335 nm. Excitation at each of the absorption peaks gave the 500-nm peak and a tiny emission peak around 600 nm. In contrast to wild-type DsRed, incubation at 37 °C did not shift the emission spectrum to a longer wavelength (data not shown).

Wild-type *Aequorea* GFP has a bimodal excitation spectrum with peaks at 395 and 475 nm. Underlying the two maxima are protonated and deprotonated states of Tyr66, which forms part of the chromophore (*2*). Because the corresponding amino acid of the chromophore-forming triad in DsRed is also a tyrosine residue, we examined the pH-sensitivity of DsRed. Emission of $DsRed_{37,75,s}$ at 583 nm was stable between pH 5 and 11 (Figure 3). $R_{500/583}$ was not altered either when the emission spectra of $DsRed_{RT,24,p}$ were measured at various pHs.

Size-Exclusion Chromatography for DsRed Expressed in E. coli. $DsRed_{RT,24,p}$ was applied to Superdex 200, a size-exclusion column (Amersham Pharmacia), and chromatograms were acquired by monitoring the absorption at 280 nm (A_{280}) for total protein, the absorption at 560 nm (A_{560}), and the fluorescence at 580 nm with excitation at 560 nm ($F_{580/560}$) for the main fluorescence component. A single peak at 13.9 mL was detected on all three traces (Figure 4A). The same chromatogram was obtained using $DsRed_{37,75,s}$ and DsRed-mu43 (data not shown). The fluorescence spectra of the peak fraction in Figure 4A and of $DsRed_{RT,24,p}$ were compared (Figure 4A, inset). The comparison indicated the

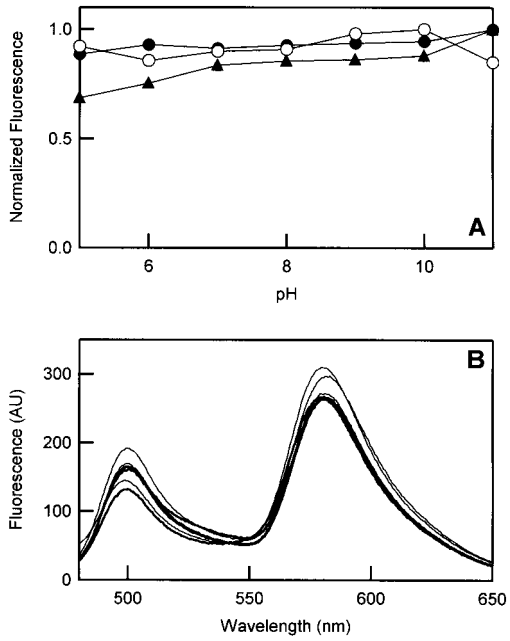

FIGURE 3: pH-dependency of the fluorescence of DsRed. (A) Emission intensities at 583 nm with excitation at 558 nm for $DsRed_{37,75,s}$ (open circles) and $DsRed_{RT,24,p}$ (closed circles), and emission intensities at 500 nm with excitation at 460 nm for $DsRed_{RT,24,p}$ (closed triangles) were measured at various pHs. Data were normalized with the highest values of respective samples. (B) Emission spectra of $DsRed_{RT,24,p}$ at various pHs obtained by excitation at 460 nm. Buffers used were phosphate (pH 11), glycine−NaOH (pH 10, 9), HEPES−NaOH (pH 8), MOPS−NaOH (pH 7), MES−NaOH (pH 6), and sodium acetate (pH 5).

main component and subcomponent not to be separable from each other by hydrodynamic behavior. We treated $DsRed_{37,75,s}$ with enterokinase to remove the Xpress tag, which might contribute to complex formation. Liberation of the tag was confirmed by SDS−PAGE followed by CBB staining (Figure 4B, inset). The tag-free DsRed was eluted at 14.6 mL (Figure 4B), and its apparent molecular mass was estimated to be 75.6 kDa.

Next, we determined the absolute molecular mass of $DsRed_{37,75,s}$ using a multiangle light scattering analysis. We applied the enterokinase-treated sample onto two size-exclusion columns that were tandemly connected (KW-804 and KW-803, Shodex), and analyzed the eluate using a multiangle laser light scattering photometer (Figure 4C). The absolute molecular mass was calculated to be 114.7 kDa. This value was 4.37 times larger than that (26.24 kDa) deduced from the primary structure of the enterokinase-treated DsRed. It was therefore concluded that the DsRed expressed in bacteria forms a homotetrameric complex. Since the same elution pattern was obtained with $DsRed_{RT,24,p}$ and DsRed-mu43 as well as $DsRed_{37,75,s}$, and even when the samples were diluted to 3.3 nM, the tetramer complex should be stable, irrespective of the fluorescence property or maturation state.

Expression of DsRed in Mammalian Cells. Based on the temperature-dependent maturation of DsRed, we speculated that the maturation of red fluorescence might proceed efficiently in mammalian cells, which are usually kept at 37 °C. First, we studied how soon the fluorescence appeared in cell extracts from HeLa cells that had been transfected with DsRed/pcDNA3. Figure 5A shows emission spectra of the

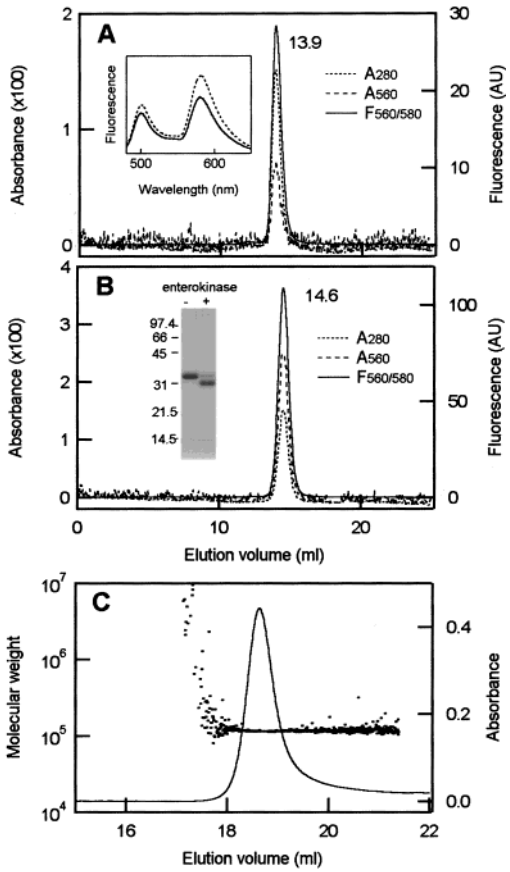

FIGURE 4: Size-exclusion chromatography of DsRed. $DsRed_{RT,24,p}$ (A) and enterokinase-treated $DsRed_{37,75,s}$ (B) were applied onto Superdex 200, and chromatograms were obtained by monitoring A_{280}, A_{560}, and $F_{560/580}$. The inset in (A) shows emission spectra of $DsRed_{RT,24,p}$ (dotted line) and of the fraction corresponding to the 13.9-mL peak (solid line), acquired with excitation at 460 nm. The inset in (B) shows band patterns of $DsRed_{37,75,s}$ before and after the enterokinase treatment on SDS−PAGE followed by CBB staining. (C) Determination of the absolute molecular weight of the enterokinase-treated $DsRed_{37,75,s}$. The molecular weight was calculated from data of MALS and overlaid on the chromatogram of A_{280}.

cell extracts prepared 24, 48, and 72 h after transfection, which were excited at 460 and 558 nm. The main component (emission around 583 nm) emerged between 24 and 48 h after transfection, while the subcomponent (emission around 500 nm) was undetectable. The extract at 72 h post-transfection was subjected to size-exclusion chromatography with monitoring of $F_{560/580}$ (Figure 5B). Eluates were fractioned and subjected to immunoblotting analysis using an anti-DsRed antibody. Although three peaks (8.1, 14.7, and 21.8 mL) were seen on the chromatogram, only the peak at 14.7 mL was shown to contain DsRed. This position was similar to that (14.6 mL) of the bacterially expressed DsRed that was treated with enterokinase.

HeLa cells were cotransfected with DsRed/pcDNA3 and ECFP/pcDNA3. The fluorescence was observed using two-photon excitation microscopy with a 1047-nm pulse laser (Coherent) for DsRed and with an 800-nm pulse laser (Tsunami) for ECFP (Figure 6A,B). Although both DsRed and ECFP were apparently distributed throughout the cells, there was a slight difference in that the red fluorescence was observed evenly in the cytosol and nucleus, whereas the cyan fluorescence was slightly concentrated in the nucleus. When fused to calmodulin (CaM), the difference in distribution

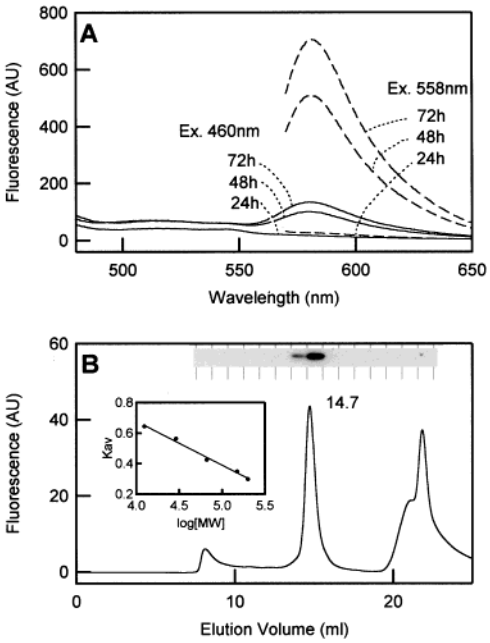

FIGURE 5: Emission spectra and size-exclusion chromatograms of DsRed expressed in HeLa cells. (A) Cell extracts were prepared 24, 48, and 72 h after transfection, and their emission spectra were acquired with excitation at 460 and 558 nm. (B) The cell extract prepared after 72 h transfection was applied onto Superdex 200, and the red fluorescence was monitored ($F_{560/580}$). The fractions were immunoblotted using anti-DsRed antibody. (B, inset) Calibration curve for the size-exclusion chromatography. Standards used are β-amylase (200 kDa), alcohol dehydrogenase (150 kDa), albumin (66 kDa), carbonic anhydrase (29 kDa), and cytochrome *c* (12.4 kDa).

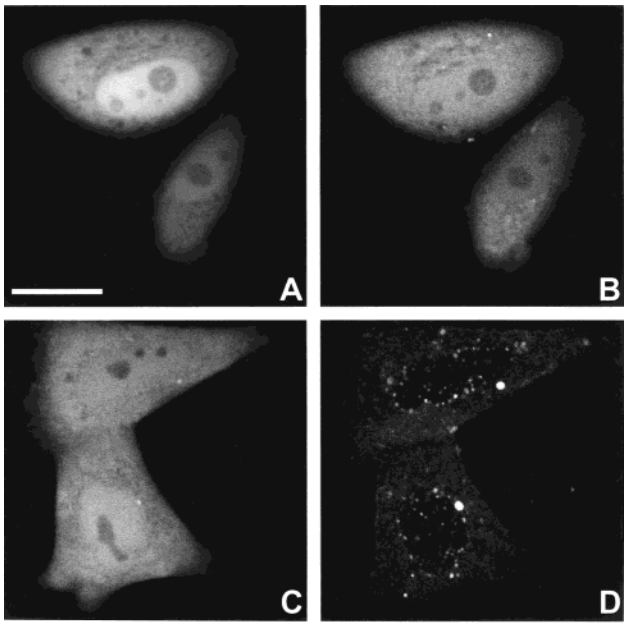

FIGURE 6: Distribution of DsRed and DsRed−CaM expressed in HeLa cells. Cells coexpressing ECFP and DsRed (A, B) or ECFP−CaM and DsRed−CaM (C, D) were imaged using a laser scanning microscope. Excitation beams for ECFP (800 nm, Ti:sapphire laser) and DsRed (1047 nm, Nb:YLF laser) were alternately irradiated. Images for ECFP were acquired through BA465-495 (A, C) and for DsRed through 590DF35 (B, D). The bar shown in (A) indicates 20 μm.

between DsRed and ECFP was remarkable (Figure 6C,D). Regardless of CaM, the same distribution of cyan fluorescence was observed. By contrast, the fluorescence of DsRed−CaM showed many spots scattered over the cytosol, suggesting aggregation of the chimera proteins.

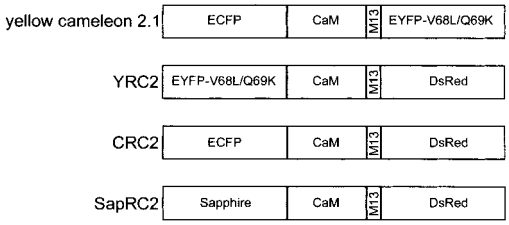

FIGURE 7: Schematic structures of yellow cameleon-2.1, YRC2, CRC2, and SapRC2.

Expression of Red Cameleons in HeLa Cells. Three red cameleons were constructed (Figure 7): yellow red cameleon-2 (YRC2), cyan red cameleon-2 (CRC2), and Sapphire red cameleon-2 (SapRC2). These camelons contained DsRed as the acceptor and EYFP-V68L/Q69K, ECFP, and Sapphire, respectively, as the donor. All the red cameleons had intact CaMs, and thus exhibited a relatively high affinity for Ca^{2+} ($K'_d = 0.2-0.4$ μM; data not shown). We expressed the red cameleons in HeLa cells and obtained sectional images of $[Ca^{2+}]_c$. Selective excitation of the donor GFP over the acceptor DsRed was attempted using a 488-nm beam argon laser for YRC2 and using a mode-locked titanium−sapphire laser with wavelengths of 770 and 800 nm for SapRC2 and CRC2, respectively. The laser power was tuned to produce sufficient fluorescent signal from the donors. The red cameleons were distributed evenly in the cytosol, with no signs of aggregation. Transient rises in $[Ca^{2+}]_c$ were observed when the cells were stimulated with histamine (10 μM). However, the emission ratios of YRC2 (Figure 8A) and CRC2 (Figure 8B) gradually fell to levels that were below the prestimuli baselines. By contrast, the emission ratio of SapRC2 rose and fell reversibly (Figure 8C). Thus, meaningful R_{max} and R_{min} values were obtained in the experiments using SapRC2.

Red Cameleons Expressed in Primary Neurons. YRC2 and SapRC2 were expressed in dissociated hippocampal neurons, in which not only elevation in $[Ca^{2+}]_c$ but also decrease in intracellular pH occurs by glutamate and/or depolarization stimuli. Imaging was performed using a conventional microscope. Figure 9A shows the spontaneous oscillation in $[Ca^{2+}]_c$ observed in a neuron expressing YRC2. The neuron was connected with several other neurons, and oscillatory changes in $[Ca^{2+}]_c$ occurred synchronously in all the neurons. The oscillations were augmented when the neurons were stimulated with 1 μM glutamate and suppressed by the application of 1 μM TTX. A slight drop in the baseline of donor signals (the fluorescence of EYFP-V68L/Q69K) was observed after glutamate stimulation (Figure 9B). Transient changes in $[Ca^{2+}]_c$ induced by depolarization were compared in YRC2-expressing and SapRC2-expressing neurons. The application of 20 mM KCl was shown to decrease the intracellular pH by 0.2−0.4. In addition to the Ca^{2+} response, the fluorescence of EYFP-V68L/Q69K (the donor of YRC2) was suppressed for over 300 s (Figure 10B), whereas no long-term effects on the fluorescence of DsRed were observed. Therefore, the decay in the $[Ca^{2+}]_c$ transient was judged to be very slow (Figure 10A). In contrast, the fluorescent signals of Sapphire and DsRed changed reciprocally (Figure 10D), and the emission ratio of SapRC2 quickly returned to the basal level (Figure 10C).

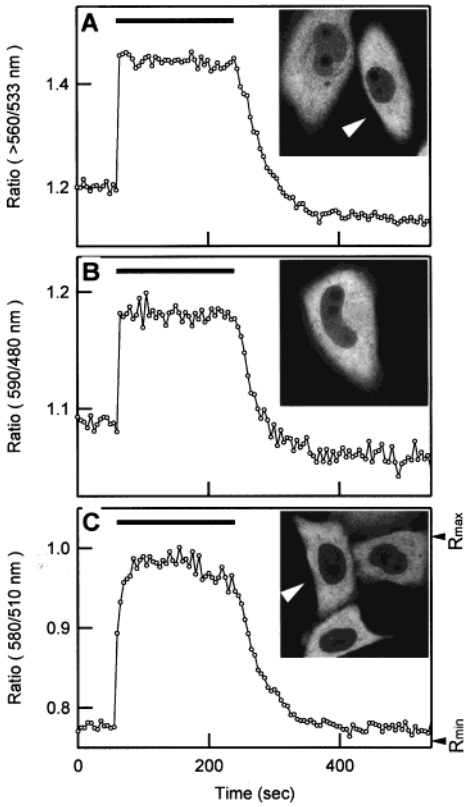

FIGURE 8: Histamine-induced $[Ca^{2+}]_c$ transients in HeLa cells expressing YRC2 (A), CRC2 (B), and SapRC2 (C). In (A) and (C), traces were obtained from cells indicated with white arrow heads. Insets show fluorescence images acquired through the donor channels described in Table 1. Perfusate was changed to buffer containing 10 μM histamine during the time indicated with bars. R_{max} and R_{min} values are indicated on the right (C).

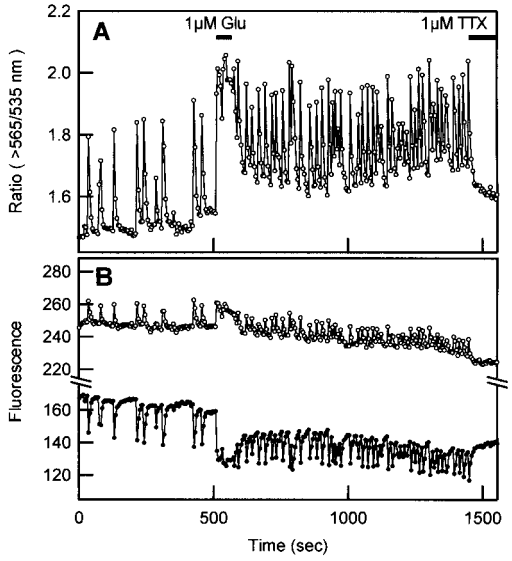

FIGURE 9: Oscillation in $[Ca^{2+}]_c$ observed in a hippocampal neuron-expressing YRC2. (A) Ratio of >565-nm to 535-nm emissions. (B) >565-nm (open circles) and 535-nm (closed circles) emissions. Perfusate was changed to buffer containing 1 μM glutamate (Glu) or 1 μM tetrodotoxin (TTX) during the time indicated in (A).

DISCUSSION

The fluorophores for multi-labels and FRET should have sharp excitation and emission spectra, allowing cross-excitation or cross-detection to be minimized. However, DsRed shows broad and complex spectra. The fluorophores

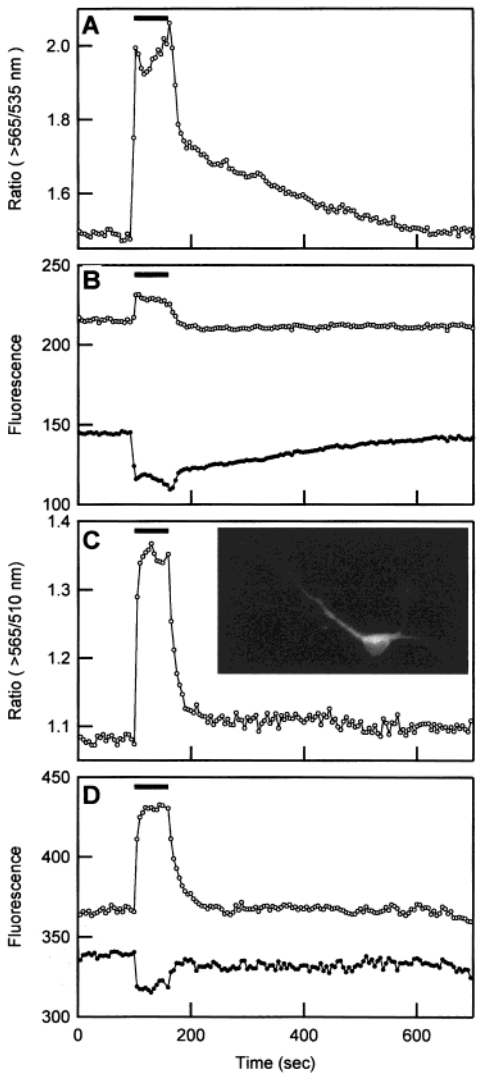

FIGURE 10: Depolarization-induced $[Ca^{2+}]_c$ transients in hippocampal neurons expressing YRC2 (A and B) and SapRC2 (C and D). The inset in (C) shows a fluorescence image of the neuron expressing SapRC2 acquired through the donor channel described in Table 2. (A) Ratio of >565-nm to 535-nm emissions. (C) Ratio of >565-nm to 510-nm emissions. (B and D) Individual emissions of acceptor (open circles) and donor (closed circles). Perfusate was changed to the buffer containing 20 mM KCl during the time indicated with bars.

functioning as fusion tags are required not to form a multimer complex; otherwise proteins with the tags might show altered functions or distributions. However, DsRed forms a stable homotetramer complex. In the present study, we investigated the spectral and structural properties of DsRed, and examined how these properties affected the usefulness of DsRed for fluorescence imaging.

Our spectral analyses revealed DsRed to have two fluorescent components: one component emitting at 583 nm, and the other emitting at 500 nm. Although the 583-nm peak is always predominant, the recombinant DsRed produced in *E. coli* at RT had a significant amount of the subcomponent emitting at 500 nm. We found that incubation at 37 °C caused a transition from green (the subcomponent) to red (the main component), thereby increasing the amplitude of the 583-nm peak, at the expense of the 500-nm peak. The temporal profile of the transition suggests that there are two states: one favors the main component, and the other the subcom-

ponent. We did not detect the shift from red to green when we incubated $DsRed_{37,75,s}$ at various temperatures and pHs. Since the transition was always unidirectional, we assume that it reflects maturation of DsRed. The more rapid maturation of DsRed at 37 °C than at RT contrasts with the better folding of *Aequorea* GFP at lower temperatures. Such a difference could be explained by the temperature of the water in which the organisms live; *Aequorea victoria* in Puget Sound vs *Discosoma* in the Indo-Pacific ocean (*3*, *15*). Although the two fluorescent components are complex, and barely separable, a comparison of the emission spectra excited at 277 nm between $DsRed_{37,75,s}$ and $DsRed_{RT,24,p}$ does give some information. The emission peak at 330 nm was less significant in the spectrum of $DsRed_{37,75,s}$ than in that of $DsRed_{RT,24,p.}$ The 277-nm light probably excites three tryptophans in DsRed (W58, W93, and W143). Since there is a spectral overlap between the emission of tryptophan and the absorption spectrum of the main component around 330 nm, the excited-state energy of the tryptophans should be used to produce the main component.

In the wild-type *Aequorea* GFP, there coexist neutral and anion chromophores, which give two absorption peaks at 395 and 475 nm. A subset of mutations has simplified the spectra to single absorption peaks at either 395 or 475 nm (*2*). We were interested in obtaining mutants of DsRed that would mature quickly. Such mutants should be purely red, and desirable for almost all cell−biological applications. However, every randomly introduced mutation slowed the maturation process. One representative mutant was DsRed-mu43 (Y120H/K168R), in which the subcomponent always predominated.

To what extent is the presence of the subfluorescent component of concern in general cell biological studies? The subcomponent was not detected in HeLa cells. Thus, DsRed proteins expressed in mammalian cells are likely to mature very rapidly, so long as the cells are kept at 37 °C. However, the rate of DsRed maturation might be regulated by factors other than incubation temperature, including the effect of fusion to other proteins. It should be noted that even without the subcomponent, the excitation spectrum of the mature DsRed (the main component) is broad. Therefore, the current DsRed suffers from cross-excitation when shorter wavelength GFPs are illuminated in multilabel and FRET experiments.

The native DsRed is composed of four polypeptide chains associated through noncovalent bonds. It is interesting to study the inter-relationships between chromophore formation and chain folding or chain association. Size-exclusion chromatography and multiangle light scattering analysis detected only one molecular species, which was the fluorescent tetrameric complex of DsRed. No intermediate species such as the monomer and dimer DsRed were observed at the protein level. These findings suggest that the synthesized DsRed protein is tetramerized very quickly. In addition, since sensitive fluorescence detection did not recognize any intermediates, DsRed probably becomes fluorescent after forming the tetrameric complex. Oligomeric association is possibly necessary for chromophore formation and maturation (the conversion from green to red). Furthermore, we did not succeed in partial or total dissociation of the DsRed complex while maintaining the fluorescence, using moderate concentrations of denaturants (8 M urea and 6 M guanidinium chloride), a detergent (1% SDS), reductants (0.1 M DTT and 0.1 M β-mercaptoethanol), and extremes of pH (pH 3). It was therefore suggested that the tetrameric complex is required to maintain fluorescence.

Generally a globular protein larger than 60 kDa is hardly able to enter the nucleus. Although DsRed forms a tetrameric complex of 115 kDa, the red fluorescence was distributed homogeneously through both the cytosol and nucleus of HeLa cell. Because the tetrameric complex species was exclusively predominant in the cell extract, it is less likely that there was an equilibrium between the tetramer and dimer or monomer, and that such small molecules passed throughout the nuclear pores. An alternative explanation is that the DsRed tetramer is not globular, but taking certain shape so that it can pass freely through the cylindrical channel about 9 nm in diameter. The peculiar structure of DsRed tetramer was suggested from its hydrodynamic behavior; size-exclusion chromatography estimated the smaller molecular mass (75.6 kDa).

In this study, we tried a differential detection of CaM-fused CFP and DsRed expressed in single cells. It was shown that CFP was selectively excited over YFP by a femtosecond-pulsed Ti:sapphire laser in the excitation wavelength range of 770−810 nm (*16*). How can we image the fluorescence of DsRed with two-photon excitation microscopy? Although it is difficult to make quantitative predictions about the behavior of two-photon absorption from the one-photon spectrum, assuming that the structure of the DsRed chromophore was not symmetrical, we expected that DsRed could be excited at the wavelength of twice the one-photon absorption maximum (558 nm). We used an Nd:YLF laser (1047 nm in 170 fs pulses at a repetition rate of 120 MHz). Two laser beams from a Ti:sapphire laser (800 nm in 80−100 fs pulses) and the Nd:YLF laser were alternately used to excite ECFP and DsRed, respectively. Then we observed that DsRed−CaM and ECFP−CaM were differently distributed in single HeLa cells. The cytoplasmic aggregation of the DsRed−CaM, however, does not necessarily mean that DsRed is inappropriate as a tag onto CaM. Making soluble fusion proteins of CaM and DsRed by switching the order of the two protein domains with various linkers is now underway.

We noticed significant bleaching of DsRed while we imaged cells using laser scanning confocal microscopy, while when HeLa cells expressing DsRed were illuminated with strong light from a xenon lamp through a 550DF30 filter (0.74 W/cm^2), the red fluorescence was not significantly bleached within 1 h (H.M., A.S., and A.M., unpublished results). Therefore, we assume that DsRed is relatively more sensitive to brief but extremely intense bursts of excitation light than to continuous-illumination light, although bleaching of fluorophore is a complex phenomenon and is related to many factors, such as light intensity, illumination time, oxygen concentrations, etc.

When DsRed is used as an acceptor for FRET, the following two characteristics of DsRed which we found in the present study should be taken into consideration.

(1) DsRed exhibits a broad excitation spectrum, even after maturation. In addition to an excitation maximum at 558 nm, several peaks and shoulders in the shorter wavelength region are present. Therefore, DsRed is not an ideal acceptor for FRET; cross-excitation of DsRed may affect the signal obtained through the FRET channel.

(2) DsRed is pH-resistant. In this respect, a pH-resistant FRET can be obtained if the donor GFP has a pH-insensitive quantum yield (*17*).

The combination of YFP and DsRed suffers from a cross-excitation of acceptors. Both the 488-nm laser beam of argon and illumination with light from a xenon lamp through a 480DF10 filter directly excited a large amount of DsRed. Therefore, the relative sensitivity to pH and light of YFP and DsRed affects the ratio value of the two emission signals. Figure 8A shows one example, in which the 488-nm laser bleached DsRed more than YFP (EYFP-V68L/Q69K) of YRC2; in another experiment using HeLa cells illuminated with the light through a 480DF10 filter, EYFP-V68L/Q69K was more bleached than DsRed of YRC2 (results not shown), suggesting again the vulnerability of DsRed to laser light. On the other hand, only EYFP-V68L/Q69K was quenched by acidification in primary neurons expressing YRC2 (Figures 9A,B and 10A,B). In all cases, the emission ratio curves were disturbed. Without such cross-excitation, the bleaching and pH sensitivity of YFP would not be a concern because the decrease in the number of YFP molecules or pH-dependent changes in the absorbance of YFP would not affect the FRET efficiency (*17*).

Cross-excitation of DsRed was also seen when cells were illuminated through a 440DF20 filter and with an 800-nm beam from a pulsed laser, both of which were used with the intention of excitating CFP selectively. While ECFP was relatively photostable against the 800-nm beam from a Ti:sapphire laser, DsRed was noticeably bleached; therefore, the ratio value (590/480 nm) gradually fell (Figure 8B). Also, CFP is not an ideal donor because of its pH-sensitive quantum yield (*17*).

Sapphire is thought to be a good donor because it is resistant to pH ($pK_a = 5.5$) (*17*) and light, and exhibits a large Stoke's shift (*8*). It should be noted that DsRed is not excited by light around 400 nm, which is the most effective wavelength for exciting Sapphire. Thus, the pairing of Sapphire−DsRed would not suffer from the above-mentioned cross-excitation. Two-photon excitation using a 770-nm-pulsed laser (Figure 8C) and light through a 400DF15 filter (Figure 10C,D) produced stable baselines. Although substitution of EYFP-V68L/Q69K for EYFP reduced the pH-sensitivity of the most popular cameleons, yellow cameleons to some extent (*7*), more pH-resistant cameleons have been desired. For instance, neuronal activity gives rise to significant acidification in neuronal cells during depolarization and glutamate stimulation. Since both Sapphire and DsRed are indifferent to pH changes, the red cameleon containing the two proteins enabled the quantitative measurement of $[Ca^{2+}]_c$ in hippocampal neurons (Figure 10C,D).

A general advantage of using *Aequorea* GFP and DsRed for FRET would be that there is less interaction between the donor and the acceptor than between two *Aequorea* GFP variants. However, our MALS analysis revealed a high molecular mass (approximately 300 kDa) for the red cameleons, indicating their homotetrameric formation. Although the present study demonstrates that they can work as Ca^{2+} indicators despite the oligomerization, the use of the current DsRed as a FRET acceptor would not be suitable for monitoring intermolecular protein−protein interactions in single living cells.

ADDED IN PROOF

Three reports published following the submission of paper have characterized the biochemistry (*18*) and photophysics (*19*) of DsRed, and determined the structure of its chromophore (*20*).

ACKNOWLEDGMENT

We thank Dr. M. Nakamura and Dr. R. Ohno for acquiring MALS data, and Dr. T. Arakawa and Dr. M. Ikura for fruitful discussions.

REFERENCES

1. Hastings, J. W., and Morin, J. G. (1998) in *Green Fluorescent Protein* (Chalfie, M., and Kain, S., Eds.) pp 17−41, Wiley-Liss, Inc., New York.
2. Tsien, R. Y. (1998) *Annu. Rev. Biochem. 67*, 509−544.
3. Matz, M. V., Fradkov, A. F., Labas, Y. A., Savitsky, A. P., Zaraisky, A. G., Markelov, M. L., and Lukyanov, S. A. (1999) *Nat. Biotechnol. 17*, 969−973.
4. Ward, W. W. (1998) in *Green Fluorescent Protein* (Chalfie, M., and Kain, S., Eds.) pp 45−75, Wiley-Liss, Inc., New York.
5. Ward, W. W., Prentice, H. J., Roth, A. F., Cody, C. W., and Reeves, S. C. (1982) *Photochem. Photobiol. 35*, 803−808.
6. Miyawaki, A., Llopis, J., Heim, R., McCaffery, J. M., Adams, J. A., Ikura, M., and Tsien, R. Y. (1997) *Nature 388*, 882−887.
7. Miyawaki, A., Griesbeck, O., Heim, R., and Tsien, R. Y. (1999) *Proc. Natl. Acad. Sci. U.S.A. 96*, 2135−2140.
8. Heim, R. (1999) *Methods Enzymol. 302*, 408−423.
9. Cadwell, R. C., and Joyce, G. F. (1992) *PCR Methods Appl. 2*, 28−33.
10. Heim, R., and Tsien, R. Y. (1996) *Curr. Biol. 6*, 178−182.
11. Wyatt, P. J. (1993) *Anal. Chim. Acta 272*, 1−40.
12. Kossel, A. H., Williams, C. V., Schweizer, M., and Kater, S. B. (1997) *J. Neurosci. 17*, 6314−6324.
13. Kakinuma, Y., Hama, H., Sugiyama, F., Goto, K., Murakami, K., and Fukamizu, A. (1997) *Neurosci. Lett. 232*, 167−170.
14. Rouget, P., Le Bert, M., Borde, I., and Evrard C. (1992) in *Neuronal Cell Lines* (Wood, J. N., Ed.) pp 27−54, IRL Press, Oxford, U.K.
15. Tsien, R. Y., and Prasher, D. C. (1998) in *Green Fluorescent Protein* (Chalfie, M., and Kain, S., Eds.) pp 97−118, Wiley-Liss, Inc., New York.
16. Fan, G. Y., Fujisaki, H., Miyawaki, A., Tsay, R.-K., Tsien, R. Y., and Ellisman, M. H. (1999) *Biophys. J. 76*, 2412−2420.
17. Miyawaki, A., and Tsien, R. Y. (2000) *Methods Enzymol. 327*, 472−500.
18. Baird, G. S., Zacharias, D. A., and Tsien, R. Y. (2000) *Proc. Natl. Acad. Sci. U.S.A. 97*, 11984−11989.
19. Heikal, A. A., Hess, S. T., Baird, G. S., Tsien, R. Y., and Webb, W. W. (2000) *Proc. Natl. Acad. Sci. U.S.A. 97*, 11996−12001.
20. Gross, L. A., Baird, G. S., Hoffman, R. C., Baldridge, K. K., and Tsien, R. Y. (2000) *Proc. Natl. Acad. Sci. U.S.A. 97*, 11990−11995.

BI002263B